

A Method for Generating Arbitrary Optical Signal Constellations Using Direct Digital Drive

Yossef Ehrlichman, Ofer Amrani, and Shlomo Ruschin

Abstract—A digitally operated optical quadrature-amplitude modulation (QAM) modulator based on a single multielectrode Mach–Zehnder modulator is presented. Generation and performance of 64QAM are studied in detail. Simulation results show that a single modulator with 13 electrodes, each of which is driven by either one of the voltages 0 or $1.68v_\pi$, provides close-to-ideal 64QAM constellation despite the inherent nonlinearity of the modulator. Moreover, employing a sufficient number of electrodes, close to ideal error performance can be obtained for any constellation order, or shape. Simulations results are demonstrated for several different square constellations: 16QAM and 256QAM, and nonsquare constellations: 32QAM and 128QAM. A brief discussion on the utilization of the proposed scheme as a predistorter is also given.

Index Terms—Direct digital drive, Mach–Zehnder, quadrature amplitude modulation (QAM).

I. INTRODUCTION

MODULATION schemes such as binary phase-shift keying (PSK) and quadrature PSK (QPSK) are typically limited to transmitting a few tens of gigabits per second on a fiber-optic channel. Approaching the 100 Gb/s range with differential-QPSK modulation would require a high signaling rate of 50 GBaud (or 25 GBaud if polarization multiplexing is used). To alleviate this problem, multilevel modulation schemes, such as M-ary quadrature amplitude modulation (QAM) (or multiphase modulation such as M-PSK) can be used. QAM is a modulation scheme that conveys data by means of modulating both the amplitude and the phase of a sinusoid carrier, thus providing spectral efficiencies in excess of 2 bit/symbol.

A widely accepted approach for generating multilevel signaling is by employing two parallel Mach–Zehnder modulators (MZMs) making the optical equivalent of an IQ modulator [1], [2]. According to this approach, the required number of control voltages increases as the number of levels in the M-ary modulation scheme is increased. For example, a 64QAM modulator may require as many as 128 distinct control voltage levels.

Ho and Cui [3] proposed a method for generating QAM signals using a single dual-drive modulator with a single electrode on each arm. Although the hardware saving associated with this

approach appears attractive, the set of distinct voltage levels required to drive the electrodes increases with the constellation size.

Kametani *et al.* [4] demonstrated the generation of 16QAM constellation with a dual-drive MZM. This modulator employs a symbol mapper comprising of a lookup table (LUT) that feeds two digital-to-analog converters (DAC) which in turn drive the two electrodes. It is shown that a driving voltage of $V_{\text{peak-to-peak}} = 1.62v_\pi$ is sufficient for covering the electric field required for ideal 16QAM modulator with a two 6-bit DACs. A limiting factor associated with this approach is the speed of the electrical DAC.

Multilevel electrical driving signals are difficult to obtain at high data rates as their implementation requires high-speed DAC. Hence, modulator configurations that rely on binary electrical driving signals are highly attractive.

Yamazaki *et al.* [5] demonstrated generation of 64QAM modulation providing 60 Gb/s. The modulator consisted of 12 high-speed phase modulators integrated with a hybrid configuration of silica planar lightwave circuits and LiNbO₃.

Siemetz [6] discussed a scheme that generates square 16QAM constellation using binary driving signals. The scheme consisted of an IQ modulator followed by a QPSK modulator, which was implemented by two phase modulators. This implementation is rather quite complex as it requires synchronizing four modulators.

Sakamoto *et al.* [7] demonstrated modulation of 16QAM at 50 Gb/s using a multiarm MZM. According to this approach, QAM signals were synthesized from binary electric signals by using a multiparallel modulator. In each arm of the modulator, binary-PSK was generated by the MZM and every two arms were paired to form QPSK. The QPSKs created in the multiparallel modulator have different amplitudes. To create 4^n -level QAM, superposing n sets of the QPSKs was required. For the generation of a 16QAM constellation, four integrated MZMs are needed, and for 64QAM constellation, six integrated MZMs are needed.

Kang [8] presented a hybrid integrated modulator using an array of four AlGaInAs/InP electroabsorption modulators (EAM) integrated with an array of semiconductor optical amplifiers to compensate for optical coupling losses. 50 Gb/s QPSK was demonstrated and it was pointed out that the modulator is capable of generating QAM signals. Doerr [9] showed a compact InP 16QAM modulator which employed four EAMs modulators using a four-arm interferometer. Lu *et al.* [10] demonstrated a 40 Gbaud 16QAM transmitter using tandem IQ modulators driven by four separate binary electrical signals.

Herein, we present a simple method for generating arbitrary M-ary constellations by introducing the concept of *direct digital driving*, which facilitates the use of only two voltage levels for

Manuscript received December 27, 2010; revised April 04, 2011, June 06, 2011; accepted June 13, 2011. Date of publication June 27, 2011; date of current version August 17, 2011.

The authors are with the School of Electrical Engineering, Tel-Aviv University, Tel-Aviv 69978, Israel (e-mail: syos@eng.tau.ac.il; ofera@eng.tau.ac.il; ruschin@eng.tau.ac.il).

Color versions of one or more of the figures in this paper are available online at <http://ieeexplore.ieee.org>.

Digital Object Identifier 10.1109/JLT.2011.2160449

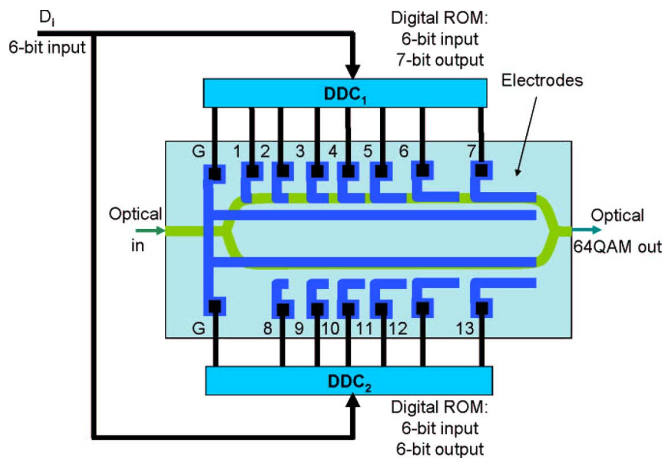


Fig. 1. 64QAM modulator based on a single multielectrode MZM. As an input, the QAM modulator accepts a 6-bit digital input word, denoted D_i . The input word is mapped by two DDC onto each of the 13 (electrode) segments, whose lengths (per arm) follow a divide-by-two sequence.

controlling each of the electrodes. Furthermore, the modulator is composed of a single multielectrode MZM.

The rest of this paper is organized as follows. In Section II, we give some basic definitions and then provide a mathematical description of the proposed modulator. The structure of the modulator is discussed in detail with there respect to a 64QAM constellation. Section III is concerned with various aspects related to the design of the modulator such as the number of electrodes and the binary driving voltage levels. The error-vector magnitude (EVM) is employed as a measure of accuracy of a generated set of points with respect to the ideal set. Section IV discusses the construction of various constellation orders. Section V briefly discusses the utilization of the proposed scheme as a predistorter. Finally, Section VI summarizes and concludes this paper.

II. GENERATION OF M-ARY CONSTELLATIONS USING A SINGLE MZM WITH DIRECT DIGITAL DRIVE

The role of an M -ary modulator is to generate a specified constellation of points which is composed of M distinct complex points (also refereed to as *signals*); the constellation points can be generally formulated as follows:

$$s_i = r_i e^{j\theta_i}, \quad r_i > 0, \quad 0 \leq \theta_i \leq 2\pi, \quad i = 1, \dots, M. \quad (1)$$

The proposed modulator is described by means of an example: Fig. 1 depicts a 64QAM optical modulator based on a single MZM whose two arms are equipped with multiple electrodes. The electrodes in this example are divided into two segments: seven electrodes on the top arm, and six on the bottom arm. Note that the center electrodes provide common ground for the active electrode segments.

As an input, this modulator accepts a 6-bit digital (electrical) word, denoted D_i . The input word is mapped onto each of the 13 electrodes via two *digital-to-digital converters* (DDC). One DDC outputs 7-bits that control the top segment of electrodes, while the other DDC controls the bottom segment. Thus, each electrode is driven by one of two voltage levels, 0 and v , representing binary 0 and 1, respectively. Eventually, these two

DDCs can be replaced by a single one with 13 output bits properly split between the two sets of electrodes. The aforementioned description suggests that the DDC can be viewed as a (high speed) digital LUT. There are various known approaches for implementing high-speed LUT (see e.g., [11]).

More generally, let $\mathbf{L}^{(1)} = (L_1^{(1)}, L_2^{(1)}, \dots, L_{N_1}^{(1)})$ and $\mathbf{L}^{(2)} = (L_1^{(2)}, L_2^{(2)}, \dots, L_{N_2}^{(2)})$ be two vectors of dimensions N_1 and N_2 , whose elements correspond to the lengths of the electrodes of the top arm and the bottom arms respectively. Let $\mathbf{B}^{(1)}$ be a binary $M \times N_1$ matrix. Row i of $\mathbf{B}^{(1)}$, $B_i^{(1)}$, holds the mapping from input D_i onto the N_1 electrodes of the top arm. Likewise, binary matrix $\mathbf{B}^{(2)}$, of dimensions $M \times N_2$, holds the mappings from each of the input digital words to the bottom N_2 electrodes. With this nomenclature, the output of the modulator can be formulated as a function of the digital input D_i as follows:

$$E_{\text{out}}(D_i) = \frac{1}{\sqrt{2}} E_{\text{in}} \exp \left\{ j\pi \frac{v}{v_\pi} \sum_{j=1}^{N_1} B_{ij}^{(1)} L_j^{(1)} \right\} + \frac{1}{\sqrt{2}} E_{\text{in}} \exp \left\{ -j\pi \frac{v}{v_\pi} \sum_{j=1}^{N_2} B_{ij}^{(2)} L_j^{(2)} \right\} \quad (2)$$

where E_{in} denotes the amplitude of the optical field entering the modulator, and v_π denotes the so-called *half-wave voltage*.¹ By setting $v = 2v_\pi$, and normalizing the summations to span $0 \leq \sum_j B_{ij}^{(1),(2)} L_j < 1$, each arm induces a phase shift of $0 \leq \Delta\phi < 2\pi$ on the optical field. Note that the matrices $\mathbf{B}^{(1)}$ and $\mathbf{B}^{(2)}$ correspond to the aforementioned LUT, while $2v_\pi \mathbf{B}^{(1)}$ and $2v_\pi \mathbf{B}^{(2)}$ fully describe the operation of the top and bottom DDCs, respectively.

Since the application of the electrical signals is directly upon the electrodes, which avoids undesirable mediating circuitry, we refer to this approach as *Direct Digital Driving*. The proposed modulator can be viewed as an extension of the 1-D DAC based on a single multielectrode MZM [12]. It acts as a 2-D DAC, which converts a digital word into an optical amplitude/phase-modulated signal.

III. MODULATOR DESIGN

The design of the modulator involves the setting of electrode lengths $\mathbf{L}^{(1)}$, $\mathbf{L}^{(2)}$, and DDC mappings $\mathbf{B}^{(1)}$, $\mathbf{B}^{(2)}$, for accurately generating the required set of signals given by (1). An analytical solution for this optimization problem, subject to various constraints has been discussed in an earlier publication [13]. Nevertheless, it can also be achieved using a simple and more straightforward numerical way.

It follows from (2) that a multielectrode MZM having N_1 electrodes on one arm, and N_2 on the other, is capable of generating at most $2^{N_1+N_2}$ distinct signals assuming (binary) direct digital drive is employed. The total number of electrodes ($N_1 + N_2$) required for generating M distinct points should satisfy $M \leq 2^{N_1+N_2}$. Practically, equality rarely suffices. From this pool of $2^{N_1+N_2}$ points, M^2 points are drawn such that they provide the closest set of points to the ideal M-QAM. By increasing the number of electrodes, a larger set of candidate output points is obtained. We shall denote this set of points as

¹This is the voltage required for inducing a phase change of π in a modulator with a single electrode of normalized length $L = 1$.

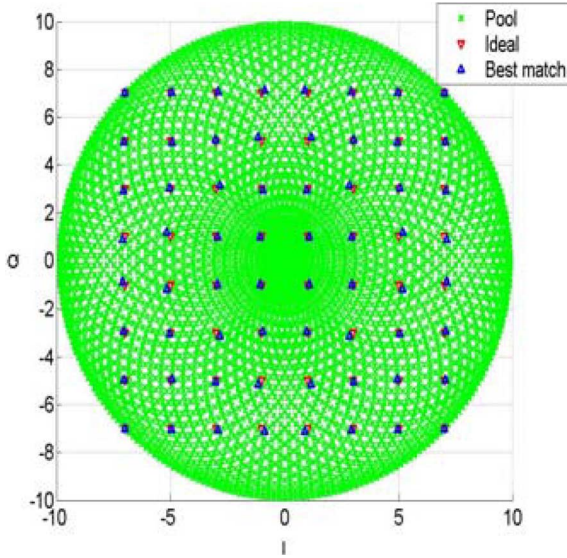


Fig. 2. Ideal 64QAM (∇); available signal pool generated using a single MZM with 7 and 6 electrodes per arm (\times); generated 64QAM constellation (Δ) (i.e., 64 points drawn from the pool).

TABLE I
ELECTRODE LENGTHS FOR $N_1 = 7, N_2 = 6$ A MODULATOR DESIGNED WITH $v_\pi L = 10$ VCM WITH INTERACTION LENGTH OF $L = 5$ CM

Top elec. [mm]	25	12.5	6.25	3.125	1.562	0.781	0.39
Bottom elec. [mm]	25	12.5	6.25	3.125	1.562	0.781	

the *signal pool*. Obviously, as the number of points in the pool is increased, the required constellation of points given by (1) can be drawn from the pool with more accuracy.

As an example, assume that a square 64QAM is the required signal constellation. Fig. 2 depicts this constellation along with a signal pool generated using $\{N_1 = 7, N_2 = 6\}$ electrodes. From this pool of 2^{13} points, 64 points are drawn (highlighted in the figure) such that they provide the closest set of points to the ideal 64QAM. As opposed to the previous publication [14], the generated constellation is spread over the entire signal pool. This improves the noise immunity of the generated constellation.

Note that the drawn set and the ideal set of points are in good agreement due to the large number of points in the pool. The 7-tuple, and 6-tuple binary vectors associated with each of the drawn points will be stored in the LUTs $\mathbf{B}^{(1)}, \mathbf{B}^{(2)}$, respectively. Hereinafter, we shall assume that the normalized electrode lengths follow a divide-by-two pattern, i.e., $L_j = 2^{-j}$.

For a modulator designed with $N_1 = 7, N_2 = 6$, and $v_\pi L = 10$ Vcm [15], then for $v_\pi = 2$ V and a total interaction length of $L = 5$ cm, the electrode lengths for each arm are given in Table I. It can be seen that the aggregate electrode length is less than 5 cm. The longest electrode will induce a phase shift of $\pi/2$ [rad] when a voltage of 4 V ($2v_\pi$) is applied to it, the second longest electrode will induce $\pi/4$, and so on. To modify the modulator to $N_1 = 7, N_2 = 7$, an additional electrode of length 0.39 [mm] is added to the bottom arm. The actual length of the

TABLE II
COMPARISON BETWEEN AN IDEAL 64QAM CONSTELLATION AND A GENERATED CONSTELLATION WITH DIFFERENT NUMBER OF ELECTRODES ON EACH ARM

64QAM					
N_1, N_2	Ideal	5,5	6,6	7,6	7,7
d_{min}	2	1.23	1.72	1.75	1.9
EVM [dB]	$-\infty$	-23.8	-31.4	-34.1	-40.3

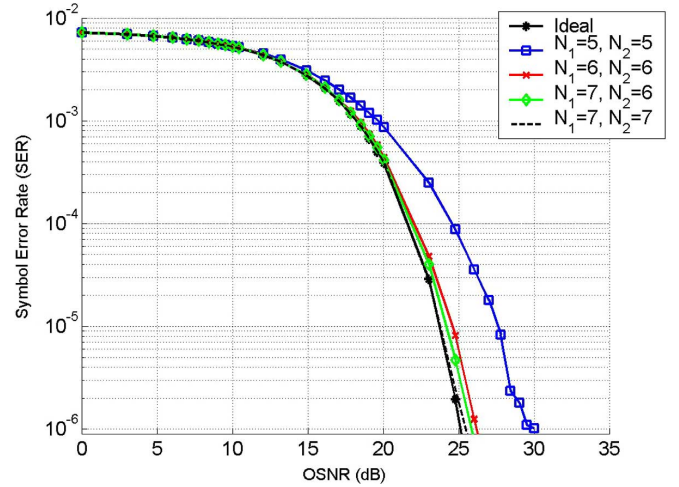


Fig. 3. SER performance curves for ideal and generated 64QAM.

modulator is bounded by the critical feature length allowed by the fabrication process.

Table II provides a comparison between an ideal (reference) 64QAM and several generated constellations using different combinations of electrodes in each arm. The table presents the minimum distance, denoted d_{min} , for each constellation along with the normalized EVM [16], which is a measure used to quantify the deviation of the generated constellation points from the ideal locations. EVM is defined mathematically as

$$EVM_{[dB]} = 10 \log_{10} \left(\frac{\sum_{i=1}^M |s_i - E_{out}(D_i)|^2}{\sum_{i=1}^M |s_i|^2} \right)$$

where s_i and $E_{out}(D_i)$ are defined in (1) and (2), respectively.

Configurations employing a smaller number of electrodes provide less than 64 different points (minimum distance of 0) and, therefore, cannot be used for generation of 64QAM.

Fig. 3 presents symbol error rate (SER) performance for an additive white Gaussian noise channel and a range of signal-to-noise ratios (SNR). It is evident that the performance quickly approach the optimal curve as the number of electrodes is increased; they practically coincides with the optimum when $\{N_1 = 7, N_2 = 7\}$. We note that optimizing the electrode lengths has very little impact on the modulator performance as observed earlier [12].

Fig. 4 shows all the possible transitions between (pairs of) the 64QAM constellation points, generated by the proposed modulator. It can be seen that there are no intensity overshoots since the peripheral constellation points are placed on the outer rim of maximum intensity. It can also be seen that the transitions are symmetric about the X -axis, but are asymmetric about the Y -axis. This asymmetry behavior means that the average about the Y axis is not zero (in signal space domain), thus producing a

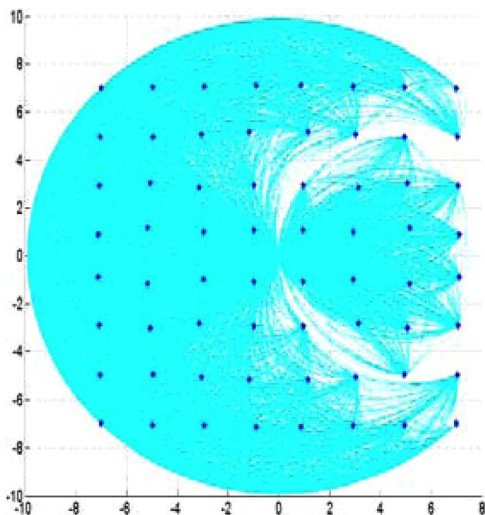


Fig. 4. All possible transitions between 64QAM constellation points generated by the proposed modulator. No intensity overshoots occur since the peripheral constellation points are placed on the outer rim with maximum intensity.

continuous-wave component in the resulting optical spectrum. The power of this spectral component will be proportional to the ratio between the transition times and the symbol time.

A. Further Design Considerations

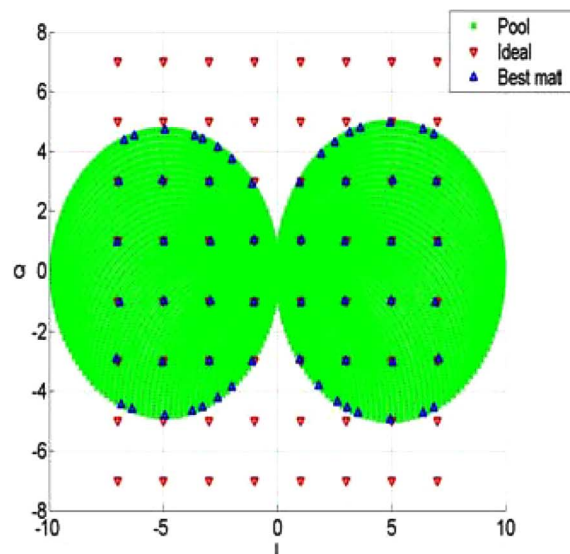
Referring to (2), it was assumed that the electrodes driving voltages are 0 and $2v_\pi$. The high-level driving voltage, corresponding to logic-1, if too high for a certain application, can be made smaller by increasing the length of the electrodes. Thus, an electrical characteristic of the device can be traded for a mechanical one. Also, (2) requires a positive phase shift on one arm and a negative phase shift on the other arm. An implementation of such a device requires either three level voltage levels, 0, $2v_\pi$, and $-2v_\pi$ or alternatively, employing dual-drive configuration as, illustrated in Fig. 1. The direction of the electric field induced by a positive applied voltage on the electrodes is toward the ground. In a modulator manufactured using Z-cut LiNbO₃ in a push-pull configuration, the electric field is applied to each arm in a different direction. Thus, for positive voltages, the phase shift in one arm increases, while the phase shift in the other arm decreases, and the device can be operated based purely on two-level electronics.

The product of the modulator driving voltage by the electrode length has a significant impact on the modulator power consumption; it is, hence, desirable to decrease this product. Table III presents the minimum distance and EVM associated with 64QAM constellation, for logic-1 driving voltages ranging from v_π to $2v_\pi$. The logic-0 driving voltage is $0v$. It can be seen that for driving voltages above $1.75v_\pi$, the minimum distance and the EVM are sufficiently close to the ideal ones (obtained with $2v_\pi$).

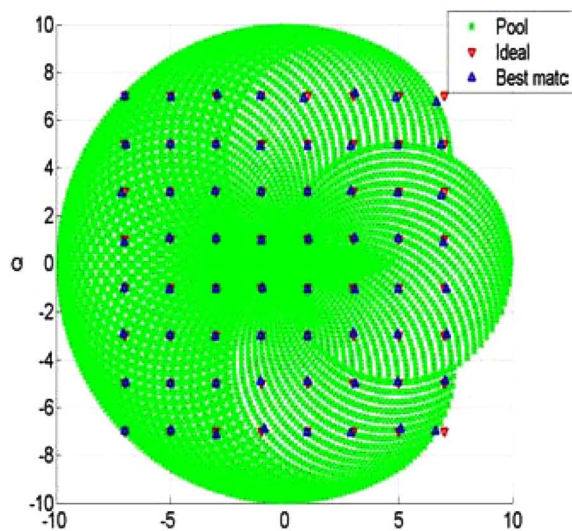
The behavior exhibited in Table III is dictated by (2). The quadrature component (the Y axis in IQ representation) is proportional to $\sin(\phi_1) - \sin(\phi_2)$, where ϕ_1 and ϕ_2 are the phase shifts induced in the upper and lower arms, respectively. In order to include the extreme points in the generated signals pool, as shown in Fig. 2, the difference should reach its maximum value of 2. This is obtained for $\phi_1 = (\pi/2)$ and $\phi_2 = (3\pi/2)$.

TABLE III
64QAM MODULATOR WITH $\{7, 6\}$ ELECTRODES PERFORMANCE FOR DIFFERENT DRIVING VOLTAGES

logic-1 driving voltage	v_π	$1.5v_\pi$	$1.68v_\pi$	$1.75v_\pi$	$2v_\pi$
d_{min}	0.45	0.36	1.54	1.67	1.75
EVM (dB)	-13.6	-23.1	-35	-34.9	-34.1



(a)



(b)

Fig. 5. Signal pool generated with 64QAM modulator for driving voltages of (a) v_π and (b) $1.68v_\pi$.

This will require an operating voltage of at least $(3v_\pi/2)$. If an operating voltage below $(3v_\pi/2)$ is used, the generated pool will appear “squeezed” and some of the 64QAM constellation points will be generated inaccurately, far from the ideal constellation points, as can be seen in Fig. 5. This will result in small minimum distance and high error rate.

It follows from Table III that the EVM for $1.68v_\pi$ and $1.75v_\pi$ is better smaller than the EVM of $2v_\pi$. Reviewing the EVM and the minimum distance for the voltage range between $1.68v_\pi$ and

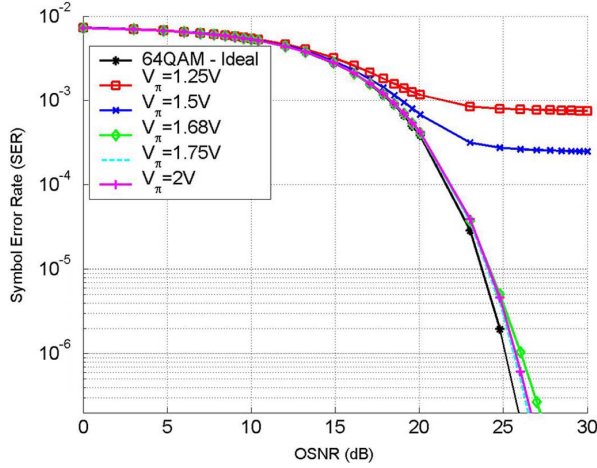


Fig. 6. SER performance curves for ideal and generated 64QAM with operating voltages of $1.25v_\pi$, $1.5v_\pi$, $1.68v_\pi$, $1.75v_\pi$, and $2v_\pi$.

$2v_\pi$ reveals that the EVM is between -34 dB and -36 dB. Fig. 6 shows the SER for ideal and generated constellations with operating voltages of $1.5v_\pi$, $1.68v_\pi$, $1.75v_\pi$, and $2v_\pi$. The SER for operating voltages greater or equal to $1.68v_\pi$ are almost identical. At SNR = 26 dB, the curve for $1.68v_\pi$ slightly diverges from the curves of $1.75v_\pi$ and $2v_\pi$. Concluding, constellations for good performance, in terms of noise immunity, can be generated with operating voltages equal or greater than $1.68v_\pi$.

IV. ON THE GENERATION OF SQUARE AND NONSQUARE QAM CONSTELLATIONS

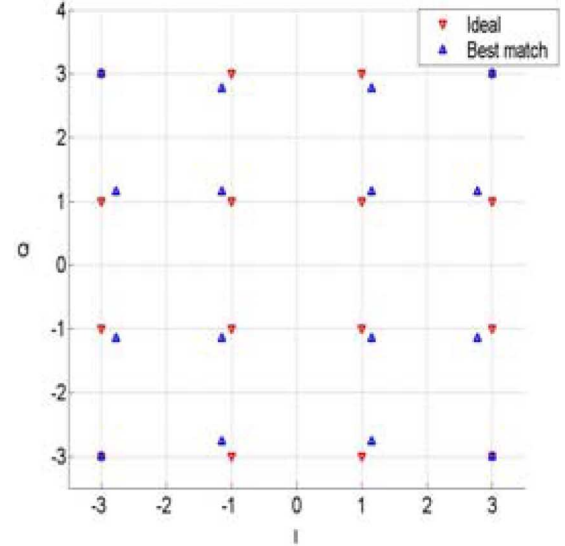
Fig. 7 presents 16QAM and 256QAM square constellations generated with $\{4, 4\}$ and $\{9, 8\}$ electrodes, respectively. The ideal constellations are also shown for reference. As the constellation order increases, the number of electrodes required for accurate generation of the signals also increases. Table IV shows the improvement in the generated constellation as the number of electrodes is increased.

Note that 256QAM can also be generated using a $\{9, 9\}$ arrangement of electrodes. Although both have 18 electrodes, this electrode setting provides slightly better performance than the $\{10, 8\}$ setting. Note that the $\{9, 9\}$ electrode setting may also be advantageous from the implementation point of view (total device length).

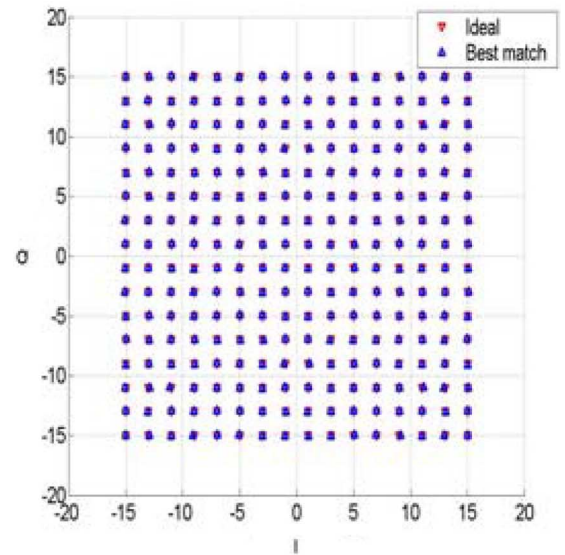
It follows that a total of nine electrodes and a total of 16 electrodes provide sufficiently accurate results for 16QAM and 256QAM, respectively.

The proposed modulator architecture can be used for generating arbitrary QAM constellations. Fig. 8 shows two non-square constellations: 32QAM and 128QAM, generated using $\{6, 5\}$, and $\{7, 7\}$, electrodes, respectively (refer to Table V). 32QAM was obtained by eliminating the four corner points of a slightly larger square constellation [$36 = (6^2)$]. Likewise, 128QAM was extracted from a square $144 = (12^2)$ constellation by removing the 16 (highest energy) points from the outer rim. The aforementioned constellations carry an integer number of bits per constellation point while maintaining a regular structure with the best energy efficiency, and are easily generated using the proposed modulator.

In practice, an optical communication system shall typically employ a single modulator for generating a wide range of con-



(a)



(b)

Fig. 7. 16QAM and 256QAM constellations using $\{4, 4\}$ and $\{9, 8\}$ electrodes, generated versus ideal.

TABLE IV
PROPERTIES OF IDEAL AND GENERATED CONSTELLATIONS AS A FUNCTION OF THE NUMBER OF ELECTRODES

16QAM					
N_1, N_2	Ideal	4,3	4,4	5,4	5,5
d_{min}	2	1.17	1.62	1.9	1.9
EVM (dB)	$-\infty$	-16	-23.18	-26.6	-26.6
256QAM					
N_1, N_2	Ideal	8,8	9,8	9,9	10,8
d_{min}	2	1.81	1.79	1.88	1.79
EVM (dB)	$-\infty$	-42.8	-46.1	-48.3	-48

stellation orders. The best constellation to be used is chosen in an adaptive manner according to instantaneous channel conditions. Clearly, as demonstrated in Table VI, a modulator tailored for generating a large constellation is expected to provide excellent accuracy for constellations of smaller order. In this ex-

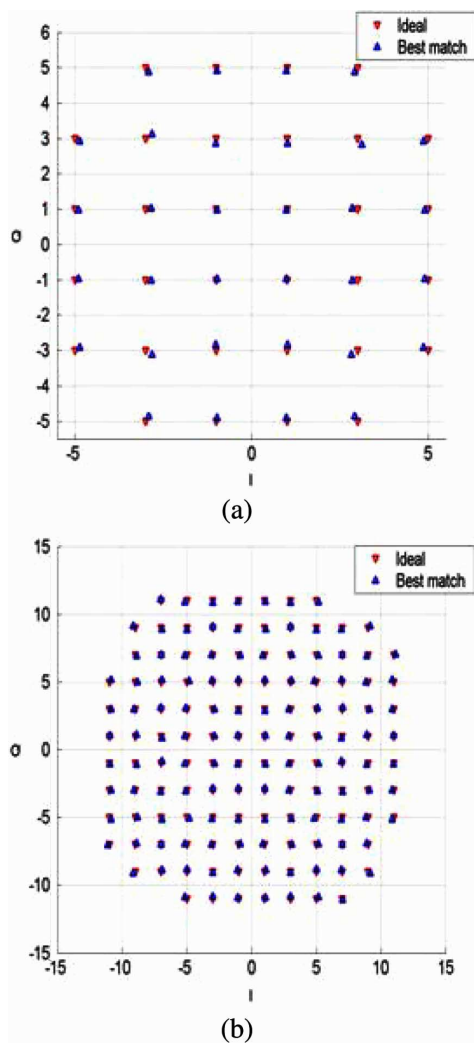


Fig. 8. Ideal and generated 32QAM and 128QAM constellations with $\{6, 5\}$ and $\{7, 7\}$, electrodes, respectively.

TABLE V
PROPERTIES OF IDEAL AND GENERATED CONSTELLATIONS AS A FUNCTION OF THE NUMBER OF ELECTRODES

32QAM			
N_1, N_2	Ideal	5,5	6,5
d_{min}	2	1.71	1.75
EVM (dB)	$-\infty$	-26.5	-30
128QAM			
N_1, N_2	Ideal	7,7	8,7
d_{min}	2	1.71	1.75
EVM (dB)	$-\infty$	-36.1	-39.5

ample, we use a $\{9, 8\}$ setting, which is sufficient. As can be seen in Table VI, the 256QAM modulator generates constellations with excellent accuracy for the lower order constellations, i.e., 16QAM and 64QAM.

V. ELECTRONIC PREDISTORTION

The use of electronic signal processing to combat optical transmission impairments due to chromatic dispersion and fiber nonlinearity offers advantages such as low cost and size, reduced optical losses, and adaptive operation. Transmission im-

TABLE VI
PERFORMANCE OF A $\{9, 8\}$ ELECTRODE SETTING USED FOR GENERATING DIFFERENT CONSTELLATIONS

$\{9, 8\}$ electrode setting			
QAM	16	64	256
d_{min}	1.97	1.91	1.79
EVM [dB]	-50	-47.3	-46.1

pairments can be mitigated at the receiver side or the transmitter side. The latter employs DSP-based techniques of electronic dispersion compensation by signal predistortion. In such techniques, the optical phase and amplitude of the transmitted signal can be controlled (predistorted) to account for various system impairments. For example, optical system impairments of the AM-to-AM (intensity-to-intensity) and AM-to-PM (intensity-to-phase) types can be mitigated by predistorting the signal prior to transmission. Previous works in that direction utilized electronic DACs, which increased system complexity and introduced additional noise to the link [17].

The proposed modulator, due to its direct digital drive architecture, requires no additional hardware for signal conversion, e.g., external DAC, for providing signal predistortion. By pre-programming the DDCs, based on knowledge of the characteristics of the system impairments and the constellation required at the receiver side, a predistorted signal can be generated. A properly predistorted signal shall propagate through the system and reach the receiver with very little distortion.

For example, a source for AM-to-PM distortion in optical fiber is self-phase modulation (SPM). SPM introduces phase shift to a modulated signal in an amount that depends (nonlinearly) on the signal power. As a result of SPM, a transmitted QAM constellation shall be received distorted: signals of different power levels shall experience different phase shift while propagating through the optical fiber.

To demonstrate the use of the proposed method, a simulation example is given for a typical fiber link whose length is 80 km. The phase shift induced on the optical signal propagating in the fiber, because of SPM, is modeled as [18]: $\phi_{NL} = 27.825 \cdot P_{in}$, where P_{in} is the average input power. Transmitting a 64QAM constellation with an input power of 6 dBm via this medium results with the distorted constellation depicted in Fig. 9(a); this is the constellation seen by the receiver (EVM = -16 dB). Fig. 9(b) depicts the received constellation (EVM = -35.6 dB) after the predistorted signal propagates through the nonlinear medium. Clearly, the received constellation closely matches an ideal 64QAM constellation. The aforementioned modulator employed a $\{7, 6\}$ electrode, but by using a $\{9, 9\}$ electrode setting (nine electrodes on each arm) the received EVM is improved to EVM = -49.7 dB.

VI. CONCLUSION

An effective modulator architecture is presented for generating arbitrary M-ary signal constellations using a single, dual-drive MZM with multiple electrodes. It is characterized by the direct digital drive approach employing two-level driving voltages. The required target performance, be it transmitter EVM or receiver BER, can be used for determining the best electrode setting $\{N_1, N_2\}$ on the arms of the MZM. Theoretically, close to ideal performance can be achieved for any constellation of discrete points by using a sufficiently large amount of electrodes.

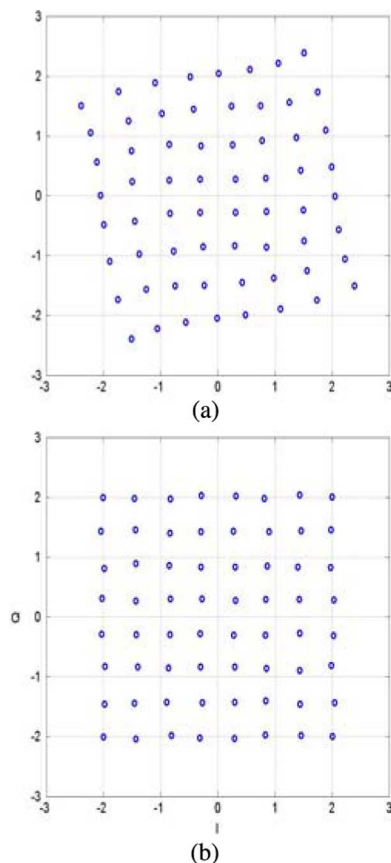


Fig. 9. (a) Distorted constellation due to SPM introduced by the optical fiber. (b) Constellation as seen by the receiver after the predistorted signal propagated through the optical fiber.

As our main example, we studied various aspects related to the generation of 64QAM. It was demonstrated that only two driving voltage levels of $0v$ and $1.68v_\pi$ are required for generating the constellation when using $\{N_1 = 7, N_2 = 6\}$ electrodes. We also briefly considered other constellation orders including nonsquare constellations such as 32 and 128QAM.

The proposed architecture can be used for combating nonlinear system impairments via predistortion. This capability is demonstrated by means of an example employing 64QAM and a typical impairment in the form of AM–PM distortion. Predistortion offers an effective method to extend transmission distances alleviating the requirements for signal recovery or optical compensation.

REFERENCES

- [1] M. Seimetz, “Multi-format transmitters for coherent optical M-PSK and M-QAM transmission,” in *Proc. 7th Int. Conf. Transparent Opt. Netw.*, Jul. 3–7, 2005, vol. 2, pp. 225–229.
- [2] E. Ip and J. M. Kahn, “Carrier synchronization for 3- and 4-bit-per-symbol optical transmission,” *J. Lightw. Technol.*, vol. 23, no. 12, pp. 4110–4124, Dec. 2005.
- [3] K. Ho and H. Cui, “Generation of arbitrary quadrature signals using one dual-drive modulator,” *J. Lightw. Technol.*, vol. 23, no. 2, pp. 764–770, Feb. 2005.
- [4] S. Kametani, T. Sugihara, and T. Mizuochi, “16-QAM modulation by polar coordinate transformation with a single dual drive Mach–Zehnder modulator,” presented at the OFC 2009, Paper OWG6.

- [5] H. Yamazaki, T. Yamada, T. Goh, Y. Sakamaki, and A. Kaneko, “64QAM modulator with a hybrid configuration of silica PLCS and LiNbO₃ phase modulators for 100-Gb/s applications,” presented at the Eur. Conf. Opt. Commun., Vienna, Austria, Sep. 20–24, 2009, Paper 2.2.1.
- [6] M. Seimetz, “High spectral efficiency phase and quadrature amplitude modulation for optical fiber transmission configurations, trends, and reach,” presented at the Eur. Conf. Opt. Commun., Vienna, Austria, Sep. 20–24, 2009, Paper 8.4.3.
- [7] T. Sakamoto, A. Chiba, and T. Kawanishi, “High-bit-rate optical QAM,” presented at the OFC 2009, Paper OWG5.
- [8] I. Kang, “High-speed photonic integrated devices for advanced modulation formats,” in *Proc. Commun. Photon. Conf. Exhib.*, 2009, pp. 1–2.
- [9] C. Doerr, “Photonic integrated circuits for high-speed communications,” in *Proc. Conf. Lasers Electro-Opt./Quantum Electron. Laser Sci. Conf.*, 2010, pp. 1–2.
- [10] G. W. Lu, M. Sköld, P. Johannisson, J. Zhao, M. Sjödin, H. Sunnerud, M. Westlund, A. Ellis, P. A. Andrekson, and P. A. A., “40-Gbaud 16-QAM transmitter using tandem IQ modulators with binary driving electronic signals,” *Opt. Exp.*, vol. 18, pp. 23062–23069, 2010.
- [11] S. Manandhar, S. Turner, and D. Kotecki, “36-GHz, 16 × 6-Bit ROM in InP DHBT technology suitable for DDS application,” *IEEE J. Solid-State Circuits*, vol. 42, no. 2, pp. 451–456, Feb. 2007.
- [12] Y. Ehrlichman, O. Amrani, and S. Ruschin, “Improved digital-to-analog conversion using multi-electrode Mach–Zehnder interferometer,” *J. Lightw. Technol.*, vol. 26, no. 21, pp. 3567–3575, Nov. 2008.
- [13] Y. Ehrlichman, O. Amrani, and S. Ruschin, “Generation of M-ary signals using a single Mach–Zehnder interferometer,” in *Proc. SPIE*, 2009, vol. 7218.
- [14] Y. Ehrlichman, O. Amrani, and S. Ruschin, “Direct digital drive optical QAM modulator with a single multi-electrode Mach–Zehnder modulator,” presented at the Eur. Conf. Opt. Commun., Torino, Italy, 2010, Paper P2.05.
- [15] K. Noguchi, O. Mitomi, and H. Miyazawa, “Millimeter-wave Ti:LiNbO₃ optical modulators,” *J. Lightw. Technol.*, vol. 16, no. 4, pp. 615–619, Apr. 1998.
- [16] M. McKinley, K. Remley, M. Myslinski, J. Kenney, D. Schreurs, and B. Nauwelaers, “EVM calculation for broadband modulated signals,” in *Proc. 64th Autom. RF Tech. Group Conf. Dig.*, 2004, pp. 45–52.
- [17] R. Killey, P. Watts, V. Mikhailov, M. Glick, and P. Bayvel, “Electronic dispersion compensation by signal predistortion using digital processing and a dual-drive Mach–Zehnder modulator,” *IEEE Photon. Technol. Lett.*, vol. 17, no. 3, pp. 714–716, Mar. 2005.
- [18] M. Seimetz, M. Noelle, and E. Patzak, “Optical systems with high-order DPSK and Star QAM modulation based on interferometric direct detection,” *J. Lightw. Technol.*, vol. 25, no. 6, pp. 1515–1530, Jun. 2007.

Yossef Ehrlichman received the B.Sc. degree in electrical engineering and the M.B.A. degree from Technion—Israel Institute Technology, Haifa, Israel, in 1999 and 2002, respectively, and the M.Sc. degree in electrical engineering from Tel-Aviv University, Tel-Aviv, Israel, in 2007, where he is currently working toward the Ph.D. degree in the field of integrated optics components for optical signal processing and optical communication.

Ofer Amrani received the Ph.D. degree in electrical engineering, from Tel-Aviv University, Tel-Aviv, Israel, in 2000.

He is currently with the School of Electrical Engineering, Tel-Aviv University. His research interests include the areas of communication and coding theory.

Shlomo Ruschin received the Ph.D. degree from the Technion, Israel Institute of Technology, Haifa, Israel, in 1977.

He was a Postdoctoral Researcher at Cornell University, Ithaca, NY. Since 1980, he is with the Faculty of Engineering, Tel-Aviv University, Tel-Aviv, Israel. His research interests include the fields of electro-optics and lasers.